

On the Role of Chain of Thought in Long Test-Time In-Context Learning

Anonymous ACL submission

Abstract

In-Context Learning (ICL) has emerged as a powerful paradigm for adapting Large Language Models (LLMs) to new tasks without gradient updates. While advances in long-context models have enabled a shift from few-shot to many-shot ICL, research has largely focused on non-reasoning tasks. Therefore, we target to address the underexplored behavior of Chain-of-Thought (CoT) prompting in many-shot scenarios, explaining the shift from studies in how to select appropriate ICL examples to how to enable LLMs to evolve their understanding at test-time. We present a comprehensive analysis of many-shot in-context CoT learning, uncovering behavioral differences between reasoning-oriented and non-reasoning oriented LLMs. Our findings show that with both types of models, there is a fundamental difference from earlier studies in the ICL setting. Crucially, we find that demonstration selection and ordering remain critically important, while semantic similarity, which is a strong heuristic for few-shot ICL and RAG, becomes ineffective. We propose that effective manyshot CoT-ICL functions as a parameter-free, test-time learning process. Supporting this, we show that (1) self-generated demonstrations (where the model creates its own training curriculum) outperform ground-truth or stronger-model demonstrations, particularly for weaker models, and (2) smoothly ordered demonstrations (measured via embedding space curvature) significantly enhance performance, mirroring principles of curriculum learning. Our findings bridge manyshot ICL with test-time scaling paradigms, reframing the context window not as a static retrieval database, but as a dynamic, structured learning environment that triggers latent model capabilities.

1 Introduction

In-context learning (ICL) enables large language models (LLMs) to perform tasks by conditioning

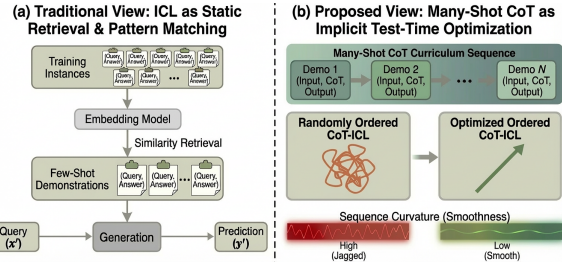


Figure 1: Reframing of CoT-ICL as test-time learning.

on a sequence of input-output demonstrations without updating their parameters (Min et al., 2022; von Oswald et al., 2023). Research has focused on improving ICL through strategies like selecting effective demonstrations (Sorensen et al., 2022; Liu et al., 2022; Wu et al., 2023). Recently, with the expansion of context windows, many-shot ICL has emerged, where dozens to hundreds of demonstrations can be provided, achieving performance competitive with fine-tuning (Agarwal et al., 2024; Bertsch et al., 2025). A consistent finding in this setting is that for non-reasoning tasks (e.g., classification), the impact of demonstration order diminishes with scale (Bertsch et al., 2025; Baek et al., 2025).

Meanwhile, chain-of-thought (CoT) prompting has become essential for complex reasoning tasks (e.g., arithmetic, narrative), where models generate intermediate reasoning steps before producing an answer (Wei et al., 2022; Kojima et al., 2022). Concurrently, the paradigm of test-time scaling investigates how to improve LLMs during inference without weight updates, through methods like sequential revision and parallel sampling (Snell et al., 2025; Lin et al., 2024). These threads connect naturally: many-shot ICL with CoT represents a fundamental form of test-time computation, where demonstrations guide the model’s behavior and understanding.

However, a critical gap exists. Our understand-

001
002
003
004
005
006
007
008
009
010
011
012
013
014
015
016
017
018
019
020
021
022
023
024
025
026
027
028
029
030
031
032
033
034
035
036
037
038
039
040

044
045
046
047
048
049
050
051
052
053
054
055
056
057
058
059
060
061
062
063
064
065
066
067
068
069
070
071
072
073

ing of many-shot dynamics derives almost entirely from studies of non-reasoning tasks. It remains unknown whether the established principles (e.g., that order matters less and similarity-based selection works) extend to many-shot CoT-ICL for reasoning. Does providing more reasoning demonstrations lead to reliable improvement, or does it introduce new instabilities? This question is practically important for deploying reasoning-capable LLMs and theoretically fundamental: it probes whether ICL for reasoning is merely large-scale pattern matching or a form of genuine in-context learning that follows pedagogical principles.

In this work, we demonstrate that the established rules of many-shot ICL break down for reasoning tasks. Through systematic experiments across model types (non-reasoning vs. reasoning-oriented) and tasks (non-reasoning vs. reasoning), our experiment uncover: (1) non-reasoning LLMs show negligible or negative gains from increasing CoT demonstrations; (2) Performance becomes more unstable with more demonstrations, indicating increased sensitivity to their order; and (3) Standard similarity-based retrieval consistently underperforms.

We explain these results by reframing effective many-shot CoT as in-context learning rather than pattern matching. We propose that successful demonstrations must be both understandable to the model and smoothly sequenced. We formalize this through two principles: (1) The Ease of Understanding: demonstrations should align with the model’s current knowledge (explaining why self-generated demonstrations work best for weaker models); and (2) The Smoothness of Knowledge Progression: the conceptual transition between consecutive demonstrations should be gradual (quantifiable via the curvature of their embedding trajectory).

Building on these principles, we introduce Curvilinear Demonstration Selection (CDS), a practical method that orders demonstrations to minimize total conceptual curvature. This approach yields an average of 3.45% performance gains across both math and narrative reasoning tasks.

Our contributions are threefold: (1) We explore the dynamic with CoT-ICL; (2) We reframe effective many-shot CoT through the lens of comprehensibility and curricular smoothness, bridging ICL with insights from test-time learning; (3) We introduce and validate a practical, principle-driven method for demonstration ordering that advances

many-shot reasoning as illustrated in Figure 1.

2 Related Works

2.1 Many-shot ICL

The extension of LLM context windows (Peng et al., 2024; Han et al., 2024) has enabled many-shot ICL, where models process significantly more demonstrations (Agarwal et al., 2024). Initial findings revealed that with sufficient demonstrations, model sensitivity to their ordering diminishes for standard classification tasks (Baek et al., 2025; Bertsch et al., 2025), suggesting a form of robustness with scaling. This led to a narrative that in many-shot settings, careful demonstration engineering may be unnecessary. However, these studies focused overwhelmingly on non-reasoning tasks (e.g., classification, simple QA) (Baek et al., 2025; Bertsch et al., 2025). Concurrent work on test-time scaling leveraging extended computation for self-improvement without parameter updates (Snell et al., 2024; Li et al., 2025), suggests that effective in-context learning can be viewed as a form of real-time optimization. Our work connects many-shot CoT-ICL to test-time learning, guided by two key principles that explain how learning occurs inside.

2.2 Chain-of-Thought

CoT prompting (Wei et al., 2022) decomposes reasoning into intermediate steps, substantially improving LLM performance on complex tasks. Subsequent studies like Tree-of-Thoughts (Yao et al., 2023) and Program-of-Thoughts (Chen et al., 2023) explore structured reasoning paths, while methods like rStar-Math (Guan et al., 2025) employ search algorithms for trajectory optimization. These approaches primarily focus on enhancing the reasoning process for a single query. In the ICL setting, Dr.ICL (Luo et al., 2023) demonstrates that retrieving relevant CoT demonstrations boosts few-shot performance. However, a critical gap remains with all existing CoT-ICL work operates in the few-shot settings. The fundamental question of how CoT demonstrations scale with context length and whether the principles of effective demonstration design change from few-shot to many-shot is largely unexplored. Our work positions many-shot CoT not merely as "more examples", but as a potential in-context curriculum that requires principled sequencing.

173 2.3 Demonstration Selection

174 Demonstration selection has long been studied for
175 effective few-shot ICL. The dominant paradigm is
176 similarity-based retrieval, where demonstrations se-
177 mantically closest to the test query are selected (Liu
178 et al., 2022; Wu et al., 2023; Kapuriya et al., 2025).
179 This approach implicitly frames ICL as a form of
180 nearest-neighbor pattern matching. Interestingly,
181 this paradigm finds a direct analogy in Retrieval-
182 Augmented Generation (RAG), where relevant con-
183 text chunks are retrieved via embedding similarity
184 (Lewis et al., 2020). Our work challenges whether
185 this conclusion extends to reasoning tasks. We
186 hypothesize that for CoT-ICL, effective demon-
187 stration selection is less about retrieving semantically
188 similar examples and more about constructing a
189 smooth learning sequence that facilitates concep-
190 tual understanding, acting as a shift from "retrieval
191 for matching" to "retrieval for learning".

192 3 Experimental Setup

193 We establish a comprehensive experimental frame-
194 work to study the factors influencing many-shot
195 Chain-of-Thought In-Context Learning (CoT-ICL).
196 Our framework focuses on three core dimensions:
197 **Tasks Type** (non-reasoning vs. reasoning), **LLMs**
198 **Type** (non-reasoning vs. reasoning LLMs), and
199 **ICL Configuration** (format and scale).

200 3.1 Tasks Studied

201 Previous studies in many-shot (Li et al., 2024;
202 Bertsch et al., 2025) have focused primarily on
203 non-reasoning tasks. We bridge this gap by eval-
204 uating a diverse set of benchmarks spanning both
205 classification and reasoning domains. All tasks
206 are formulated as open-ended text generation. The
207 model's raw output is matched against the refer-
208 ence answer or label with extra match.

209 **Non-Reasoning Tasks.** These tasks require mini-
210 mal intermediate reasoning. We include tasks with
211 varying label-space complexity, including Super-
212 GLUE (Wang et al., 2019) (narrow label space),
213 NLU (nlu, 2021), TREC (Hovy et al., 2001), and
214 BANKING77 (Casanueva et al., 2020) (large label
215 space).

216 **Reasoning Tasks.** These tasks require logical de-
217 duction and math derivation. We focus on mathe-
218 matical reasoning with GSM8K (Cobbe et al.,
219 2021) and MATH (Hendrycks et al., 2021). Addi-
220 tionally, we include DetectiveQA (Xu et al., 2025)

221 for narrative reasoning over long contexts. All
222 datasets provide ground-truth reasoning chains (C_i)
223 for deriving the answer (y_i), enabling CoT-ICL.

224 3.2 LLMs Studied

225 We compare performance of varies LLMs in long
226 context settings, categorized by their inherent rea-
227 soning design.

228 **Non-Reasoning LLMs.** These models lack a
229 dedicated internal reasoning mechanism and are
230 typically instructed-tuned for direct response,
231 including LLaMA 3.1 (Llama-3.1-8B-Instruct),
232 LLaMA 3.3 (Llama-3.3-70B-Instruct) (MetaAI,
233 2024), Qwen 2.5 (7B) (Qwen2.5-7B-Instruct) and
234 Qwen 2.5 (14B) (Qwen2.5-14B-Instruct).

235 **Reasoning LLMs.** These models are explicitly
236 trained with a reasoning token (e.g., <think>),
237 including Qwen 3 (8B) (Qwen3-8B), Qwen 3
238 (14B) (Qwen3-14B) (Yang et al., 2025) QwQ (32B)
239 (QwQ-32B) (Qwen et al., 2025) and R1 (685B)
240 (DeepSeek-R1) (DeepSeek-AI et al., 2025). For these
241 models, we enable thinking token generation dur-
242 ing inference.

243 To support the extended context required for
244 many-shot evaluations (up to 131K tokens for
245 Qwen family models), we applied official RoPE
246 scaling configuration modifications.

247 3.3 ICL Configuration

248 We study performance from few-shot to many-shot
249 under two prompting paradigms.

250 **Traditional ICL.** LLMs receives input-output
251 pairs (x_i, y_i) . Given an input x' , it generates an
252 answer $y' = \text{LLM}(x' | \{(x_i, y_i)\}_{i=1}^k)$.

253 **CoT-ICL.** LLMs receives triplets of input, rea-
254 soning chain, and output, i.e., (x_i, C_i, y_i) . Given
255 an input x' , it generates both a reasoning chain C'
256 and final answer $y' = \text{LLM}(x' | \{(x_i, C_i, y_i)\}_{i=1}^k)$.

257 **Context Scaling.** The token length of CoT-ICL
258 is substantially larger than that of traditional ICL
259 (e.g., geometry problems are about 30 times longer
260 than BANKING77 examples). Therefore, while
261 models can process hundreds to thousands of tradi-
262 tional ICL demos, the context window typically
263 limits CoT-ICL to hundreds demonstrations. Our
264 analysis focuses on this scaling range (up to 128
265 demonstrations), where we observe the most infor-
266 mative dynamics between model capability, task
267 type, and demonstration count.

268 4 Properties of CoT-ICL

269 4.1 Scaling with Non-Reasoning LLMs

270 While recent work demonstrates that many-shot
 271 ICL yields consistent gains for non-reasoning
 272 tasks (Bertsch et al., 2025; Baek et al., 2025), we
 273 find this scaling behavior does not generalize to
 274 reasoning tasks with CoT prompts. Figure 2 reveals
 275 that non-reasoning tasks exhibit steady improve-
 276 ment with more demonstrations, whereas math rea-
 277 soning performance fluctuates or declines with
 278 non-
 279 reasoning LLMs for most of the tasks (especially
 280 for math reasoning tasks).

281 This failure to scale is not simply a limitation of
 282 model size. As shown in the left subplot of Figure 3,
 283 even the 70B-parameter Llama 3.3 shows negative
 284 gains. This contrasts with the effect of scaling
 285 observed in previous many-shot ICL, suggesting a
 286 qualitative difference in how LLMs process long
 287 CoT-ICL.

288 4.2 Scaling with Reasoning LLMs

289 In contrast to non-reasoning LLMs, models with
 290 explicit reasoning capabilities exhibit a fundamen-
 291 tally different scaling pattern. As shown in right
 292 subplot of Figure 3, QwQ (32B) demonstrates clear
 293 positive scaling with additional demonstrations.
 294 This pattern holds for smaller reasoning-optimized
 295 models as well: the Qwen3 family (Figure 4) shows
 296 consistent performance gains as the number of
 297 demonstrations increases. LLMs with reasoning
 298 capabilities (enabled via thinking tokens or spe-
 299 cialized training) successfully leverage additional
 300 CoT demonstrations to improve performance on
 301 reasoning tasks. The divergence in scaling behavior
 302 between model types highlights that the ability to
 303 benefit from many-shot CoT is not merely a func-
 304 tion of pattern matching, but is intrinsically linked
 305 to a model’s capacity for in-context reasoning.

306 4.3 Instability of Many-shot CoT-ICL

307 The divergent scaling patterns suggest that the se-
 308 quence of demonstrations may be critical for CoT-
 309 ICL. To test this, we measure performance vari-
 310 ance across five random orderings of the same
 311 demonstration set. Prior work finds that vari-
 312 ance decreases with more demonstrations for non-
 313 reasoning tasks (Baek et al., 2025), indicating that
 314 order becomes less important. We observe the same
 315 for classification tasks in the left subplot in Fig-
 316 ure 5.

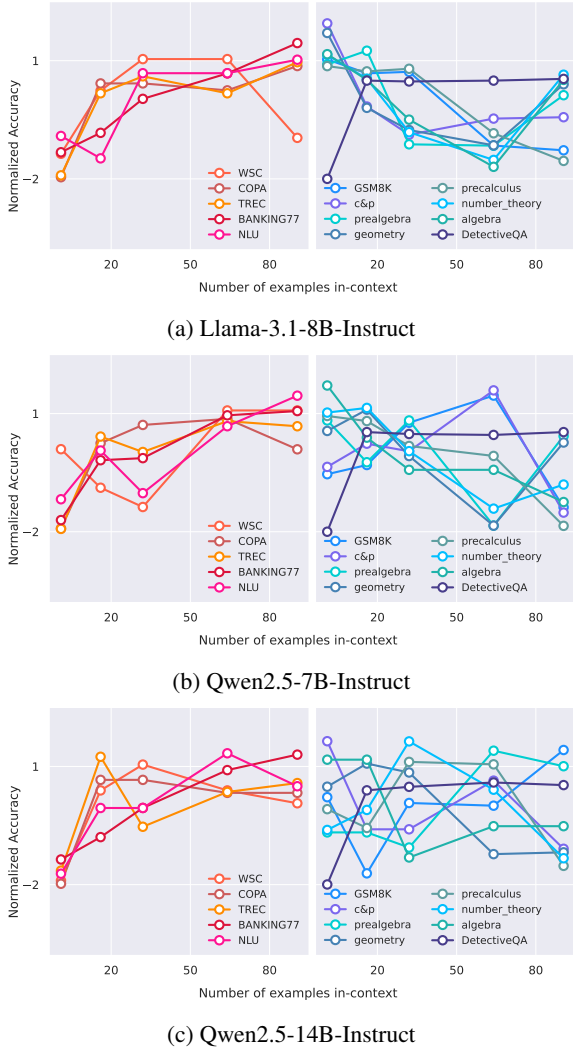


Figure 2: Scaling disparity between task types. Performance (normalized accuracy) of non-reasoning LLMs on classification tasks (**warm colors**) versus reasoning tasks (**cool colors**). The x-axis represents normalized accuracy (i.e., $\frac{x-\bar{x}}{\sigma_x}$ for accuracy x), while the y-axis indicates the number of in-context demonstrations.

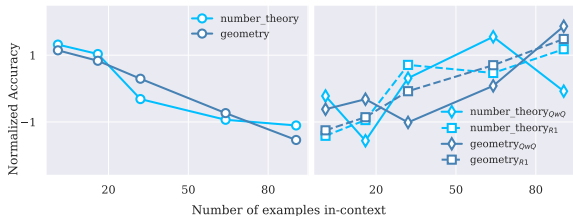


Figure 3: Scaling disparity between model types on math reasoning tasks. **Left:** Llama 3.3 (non-reasoning LLM) shows negative gains. **Right:** QwQ (32B) and R1 (685 B) (reasoning LLM) shows clear positive scaling.

316 However, for reasoning tasks with CoT, we find
 317 the opposite trend. Variance increases with more
 318 demonstrations as shown in the right subplot in

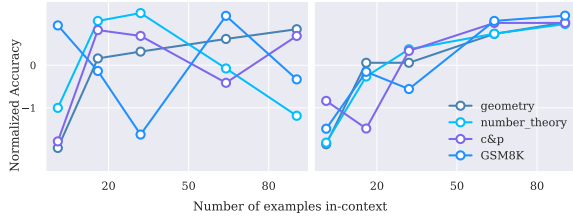


Figure 4: Positive scaling of reasoning LLMs. The Qwen3 family (reasoning LLMs) demonstrates consistent performance improvements with more demonstrations on math reasoning tasks. **Left:** Qwen3 (8B) **Right:** Qwen3 (14B)

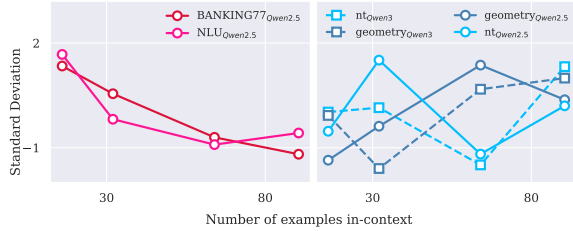


Figure 5: Standard deviation of performance across five random demonstration orders on classification tasks (**warm colors**) versus reasoning tasks (**cool colors**), where nt corresponds to number_theory. Results shown for Qwen2.5 (14B) (non-reasoning) and Qwen3 (14B) (reasoning).

319
320
321
322
323
324
325
326
327
328
329
330
331
332
333
334
335
336
337
338
339
340
341
342

Figure 5. This holds for both non-reasoning and reasoning LLMs, revealing a key instability finding: Many-shot CoT exhibits increasing sensitivity to demonstration order as context length grows, unlike non-reasoning ICL where order becomes less important.

This increasing instability indicates that simply adding more CoT examples can introduce confusing signal. The model’s performance becomes highly path-dependent, suggesting that the progression of reasoning steps across demonstrations is a critical, previously overlooked factor in CoT-ICL.

331 4.4 Rethinking the role of similarity

332 Given the importance of order, we investigate
333 whether standard retrieval heuristics can identify
334 helpful demonstrations. In few-shot ICL and
335 retrieved-augmented generation (RAG), retrieving
336 demonstrations semantically similar to the query is
337 highly effective (Liu et al., 2022; Wu et al., 2023).
338 We test this in the many-shot CoT setting using
339 Qwen3-Embedding-4B (Zhang et al., 2025) to con-
340 struct “most similar” and “most dissimilar” demon-
341 stration sets. Specifically, we construct two unified
342 sets of in-context examples: one comprising the

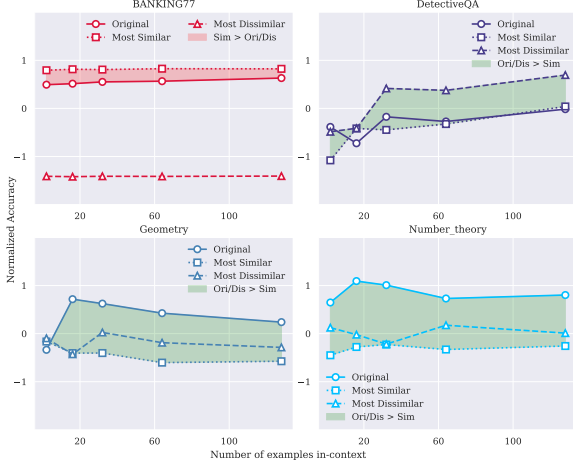


Figure 6: Performance with original(ori), similarity(sim) and dissimilar(dis) sets averaged across five LLMs. The area between the two sets is filled with colors, indicating the relative performance at each point. The normalization is performed with the mean and standard deviation computed over the concatenated sets of ori, sim and dis.

most semantically similar examples and the other comprising the most dissimilar examples to the test set. Similarity is measured by computing the cosine similarity between question embeddings, averaged across the entire test set. The training set instances form the candidate pool for constructing the similar and dissimilar example sets. Experiments are conducted and averaged over five LLMs, including Llama 3.1, Qwen 2.5 family (7B and 14B) and Qwen 3 family (8B and 14B).

The results in Figure 6 reveal an opposite pattern. For the BANKING77 classification task, similar examples outperform dissimilar ones, aligning to prior findings. For all three reasoning tasks (geometry, number_theory, DetectiveQA), the dissimilar set or the original set consistently outperform the similar set as the number of demonstrations increases. Performance for separated evaluated on reasoning and non-reasoning LLMs is in Appendix B and same conclusion is drawn when looking separately on different types of LLMs.

This failure suggests that reasoning tasks require a deeper, structural understanding of the problem space rather than surface-level pattern matching. Similar questions may cluster in solution strategy, providing redundant learning signal, while diverse (dissimilar) examples might better scaffold the model’s understanding of the reasoning process itself.

343
344
345
346
347
348
349
350
351
352
353
354
355
356
357
358
359
360
361
362
363
364
365
366
367
368
369
370
371

372 **5 Rethinking ICL: From Pattern**
373 **Matching to Test-Time Learning**

374 Our empirical findings in Section 4.3 and 4.4
375 present a puzzling contradiction, while CoT-ICL
376 shows a promising trend with manyshot, it ex-
377 hibits increasing sensitivity to demonstration or-
378 der and fails to benefit from established heuristics
379 like similarity-based selection. We propose a con-
380 ceptual shift to explain these observations: rather
381 than viewing ICL as mere pattern matching in an
382 extended context, we should conceptualize it as
383 test-time learning—a form of gradient-free opti-
384 mization occurring within the forward pass. This
385 reframing provides a principled basis for under-
386 standing what makes demonstrations effective and
387 leads us to formulate two complementary prin-
388 ciples for demonstration design.

389 **5.1 Test-Time Learning**

390 The success of simple heuristics like retrieving
391 demonstrations similar to the query in such settings
392 supports this pattern-matching view. However, our
393 findings in Section 4.3, particularly the increasing
394 variance with more demonstrations in reasoning
395 tasks and the failure of similarity-based selection,
396 directly contradict this interpretation for the many-
397 shot CoT setting.

398 We posit that when provided with many demon-
399 strations, especially those involving complex rea-
400 soning chains, the LLM engages in a more pro-
401 found form of in-context learning: it is not merely
402 recognizing a pattern, but actively constructing
403 or refining an internal "algorithm" or reasoning
404 schema based on the provided examples. This also
405 aligns with the emergent perspective of test-time
406 scaling and its effectiveness (Snell et al., 2024).

407 This learning analogy helps explain our key ob-
408 servations,

- **The importance of order:** Effective learning typically follows a curriculum—from simple to complex, or following logical progression. Random ordering disrupts this progression, leading to unstable "learning" outcomes.
- **The failure of similarity:** When learning a new concept, the most similar examples are often redundant and do not expand the model's understanding. Conversely, diverse examples that cover different facets of a problem can provide richer learning signals.

Effective demonstration selection for ICL re-
quires retrieving pedagogically useful examples,
those that facilitate learning the task itself rather
than just providing answers. Similarly, test-time
scaling methods like self-critique use multiple for-
ward passes to iteratively refine outputs; many-shot
ICL can be seen as a parallel, one-pass version
of this refinement, where multiple demonstrations
collectively shape the model's reasoning trajectory.

420 **5.2 The Ease of Understanding**

If ICL functions as test-time learning, then demon-
strations must be comprehensible to the model
within its current capabilities. Drawing from ed-
ucational psychology, effective instruction oper-
ates within a learner's "zone of proximal develop-
ment" (Benson, 2020), the space between what
they can do independently and what they can
achieve with guidance. We hypothesize that effec-
tive demonstrations must reside within the model's
"zone of understandable reasoning."

Settings. To test this principle, we investigate
whether demonstration efficacy depends more on
reasoning quality or alignment with the model's
own generative patterns. We generate CoT demon-
strations by prompting each LLM on training in-
stances and categorize them into three sets:

- **Correct Set (cr):** Model-generated CoT with correct final answers
- **Incorrect Set (wr):** Model-generated CoT with incorrect final answers
- **First Set (first):** The first generation for each instance, regardless of accuracy

These are compared against the dataset's
groundtruth CoT (i.e., origin). Each LLM is
prompted 10 times per training instance with tem-
perature=1.0 to ensure diversity. Due to high accu-
racy on GSM8K, the wr set is constructed only for
number_theory and geometry tasks. Additionally,
we evaluate whether "better" CoT from stronger
models (i.e., Qwen 2.5 (14B)) improves weaker
model performance.

Results. Figure 7 reveals that the wr set (in-
correct reasoning) consistently outperforms the orig-
inal CoT and performs comparably to the cr set
across both LLMs and tasks. This demonstrates
that distributional alignment with the model's own
reasoning style, even when flawed, contributes

more to stable CoT prompting than the presence of correct answers.

Furthermore, self-generated CoT (any of cr, wr, or first sets) significantly mitigates the instability issues observed with origin CoT. The first set, the model’s natural first attempt at each problem, also outperforms origin CoT (Figure 8), reinforcing that distributional alignment is paramount.

When using CoT from stronger models, we observe a mixed pattern: while occasional performance gains occur, instability persists (olive lines in Figures 7 and 8). This suggests that reasoning patterns too advanced for the target model can disrupt rather than enhance learning, similar to teaching advanced concepts before fundamentals.

Interpretation. These findings support that the effective demonstrations for in-context learning are those that the model can naturally comprehend and relate to its existing knowledge structures. Self-generated CoT, even when incorrect, provides such "understandable examples" by matching the model’s own reasoning distribution, facilitating more stable test-time learning. It is also related to the LLM’s internal ability to comprehend demonstration context. For demonstrations that are not understandable by LLMs (i.e., Qwen2.5 family and Qwen 3 (7B)), the benefit brings by self-generated CoT over groundtruth CoT is significant. But with a stronger LLM (i.e., Qwen 3 (14B)) that can understand well on the groundtruth CoT, this benefits shrink, as illustrated in Figure 8).

5.3 The Smoothness of Information Flow

Effective learning requires not just comprehensible individual examples, but a coherent progression between them. We hypothesize that smooth transitions between demonstrations facilitate the model’s construction of a coherent reasoning schema, while abrupt conceptual jumps disrupt this process.

Quantifying Transition Smoothness To operationalize this principle, we conceptualize the sequence of demonstration embeddings as a trajectory through semantic space. We define the curvature between consecutive demonstrations as the angle between the vectors connecting them:

$$\theta_i = \arccos \left(\frac{(\mathbf{e}_i - \mathbf{e}_{i-1}) \cdot (\mathbf{e}_{i+1} - \mathbf{e}_i)}{\|\mathbf{e}_i - \mathbf{e}_{i-1}\| \|\mathbf{e}_{i+1} - \mathbf{e}_i\|} \right) \quad (1)$$

For an ordered sequence $O = [\mathbf{d}_1, \mathbf{d}_2, \dots, \mathbf{d}_n]$ and their corresponding embedding $E =$

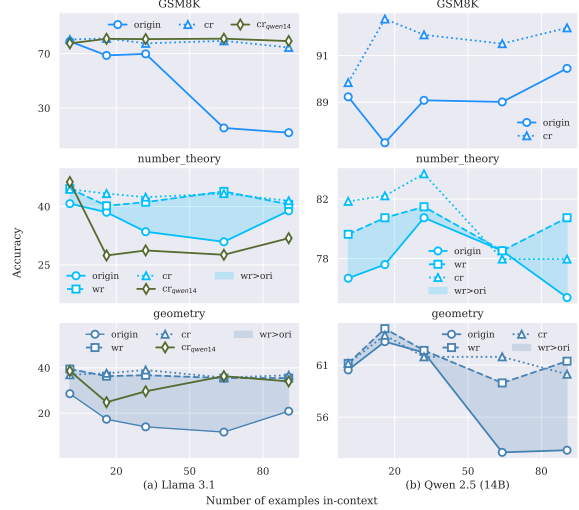


Figure 7: Performance of two sets of self-generated in-context CoT, including the set filtered with only correct answer(cr) and the set filtered with only wrong answer(wr). cr_{qwen14} is prompting the LLaMA model with the in-context CoT generated by Qwen 2.5 (14B). **Left:** Llama 3.1 **Right:** Qwen 2.5 (14B)

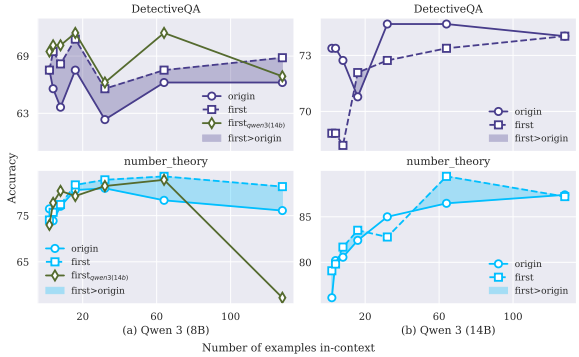


Figure 8: Performance of the first set of self-generated in-context CoT. cr_{qwen3(14b)} is prompting the Qwen 3 (8B) model with the in-context CoT generated by Qwen 3 (14B). **Left:** Qwen 3 (8B) **Right:** Qwen 3 (14B)

$\{\mathbf{e}_1, \mathbf{e}_2, \dots, \mathbf{e}_n\} \subset \mathbb{R}^d$, the total curvature $\Theta(E) = \sum_{i=2}^{n-1} \theta_i$, with lower values indicating smoother transitions between demonstrations. The detail algorithm is on Appendix A.

Dimensionality reduction for efficiency. To facilitate efficient computation of smoothness and to capture both global and local structures, as well as linear and non-linear patterns, we project the embeddings into a lower-dimensional space using PCA (Maćkiewicz and Ratajczak, 1993) and UMAP (McInnes et al., 2018). Correlation is computed with 128 number of demonstration and we set the number of component $d' = 50$.

527
528 **Projection Method:** We compute a combined
projection $P(E) \in \mathbb{R}^{n \times d'}$ as:

529
$$P(E) = \text{PCA}(E, d') + \text{UMAP}(E, d') \quad (2)$$

530
531 The PCA component $\text{PCA}(E, d')$ captures
532 global linear structure, while the UMAP com-
533 ponent $\text{UMAP}(E, d')$ preserves local nonlinear
534 relationships crucial for reasoning tasks. The PCA
projection is weighted by explained variance:

535
$$\text{PCA}(E, d') = E_{\text{pca}} \cdot \text{diag}(\sqrt{\lambda}) \quad (3)$$

536 where $\lambda = [\lambda_1, \dots, \lambda_{d'}]$ are the explained
537 variance ratios.

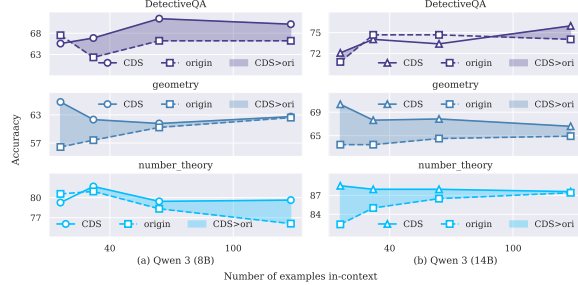
538
539 **Result.** Our analysis reveals a negative correlation
540 (r=-0.602) between ordering smoothness and
541 performance across three math reasoning tasks.
542 With the correlation of -0.654, -0.511 and -0.642
543 corresponding to geometry, number_theory and
544 counting_and_probability tasks, it supports that
545 smooth information flow facilitates effective in-
546 context learning. Additionally, the finding that
547 variance increases with more demonstrations in
548 reasoning tasks in Section 4.3 can be reinterpreted
549 as follow, With more demonstrations, the proba-
550 bility of encountering disruptive conceptual jumps
increases, leading to greater outcome variability.

551
552 **Pedagogical Analogy** This principle mirrors ef-
553 fective textbook design: concepts are introduced
554 progressively, with each chapter building smoothly
upon the previous. Abrupt topic changes or missing
555 prerequisites hinder learning. Similarly, in many-
556 shot CoT-ICL, demonstrations must be ordered to
557 create a "conceptual curriculum" that guides the
558 model from basic to advanced reasoning steps.

559 6 Curvilinear Demonstration Selection

560
561 Based on the strong correlation between curva-
562 ture and performance established in Section 5.3,
563 we now introduce Curvilinear Demonstration Se-
564 lection (CDS), a practical method for optimizing
565 demonstration ordering in many-shot CoT-ICL.
566 The core insight is that minimizing total curvature
567 along the demonstration sequence corresponds to
568 creating a smoother learning progression, analo-
569 gous to how textbooks organize chapters by gradu-
ally increasing conceptual difficulty.

570
571 **Method.** Finding the global minimizer of Θ can
572 computationally intractable for large n , but can
be effectively approximated by formulating it as a



573 Figure 9: Performance comparison between CDS or-
574 dered CoT-ICL and originally ordered CoT-ICL. **Left:**
575 Qwen 3 (8B) **Right:** Qwen 3 (14B)

576 Traveling Salesman Problem (TSP). We solve this
577 TSP using a nearest neighbor heuristic with 2-opt
578 optimization (Croes, 1958).

579 **Dimensionality reduction.** Since we cannot
580 adopt $d' = 50$ for all number of demonstrations, we
581 adopt the following strategy. For n demonstrations,
582 we set the number of components d' as:

583
$$d' = \left\lfloor \frac{n}{5} \right\rfloor \times 5 \quad (4)$$

584 This rounding to the nearest multiple of five en-
585 sures computational efficiency while maintaining
586 sufficient expressivity. For example, with $n = 128$,
587 we use $d' = 125$ components.

588 **Result.** We evaluate CDS on three challenging
589 reasoning tasks: geometry proof generation, num-
590 ber theory problem solving, and DetectiveQA log-
591 ical reasoning. Figure 9 shows the performance
592 comparison across different ordering strategies. Re-
593 sult shows that CDS outperform all baselines across
the evaluated tasks, with average improvements of
3.45%.

594 7 Conclusion

595 We have shown that many-shot chain-of-thought
596 in-context learning (CoT-ICL) does not follow the
597 same property as standard many-shot ICL. To ex-
598 plain this, we reframe the ICL from pattern match-
599 ing to in-context "learning", explained with two
600 principles. Based on these, we propose CDS,
601 a method that orders demonstrations to ensure
602 smooth conceptual transitions. Our work reframes
603 demonstration selection as a retrieval-for-learning
604 problem. By designing demonstrations that teach
605 rather than just match, we can build more robust
and capable reasoning systems.

606 Limitations

607 Due to the computational cost and performance
608 limitations of LLMs in long in-context CoT rea-
609 soning, our study is limited to approximately 100
610 examples. While LLMs like Qwen 2.5 and LLaMA
611 3.1 can handle up to 131K and 128K context to-
612 kens, respectively, their performance in in-context
613 CoT reasoning declines gradually beyond a cer-
614 tain threshold of context tokens, making exploring
615 beyond 100 shots in this setting insignificant. In
616 addition, the effectiveness of CDS depends on the
617 quality of the underlying embeddings. Though,
618 Qwen3-Embedding-4B shows a promising perfor-
619 mance on both narrative and math reasoning.

620 References

621 2021. Benchmarking natural language understand-
622 ing services for building conversational agents. In *In-*
623 *creasing Naturalness and Flexibility in Spoken Dia-*
624 *logue Interaction*, Lecture Notes in Electrical Engi-
625 *neering*, pages 165–183. Springer.

626 Rishabh Agarwal, Avi Singh, Lei M Zhang, Bernd
627 Bohnet, Luis Rosias, Stephanie C.Y. Chan, Biao
628 Zhang, Aleksandra Faust, and Hugo Larochelle. 2024.
629 **Many-shot in-context learning**. In *ICML 2024 Work-*
630 *shop on In-Context Learning*.

631 Jinheon Baek, Sun Jae Lee, Prakhar Gupta, Geunseob
632 Oh, Siddharth Dalmia, and Prateek Kolhar. 2025.
633 **Revisiting in-context learning with long context lan-**
634 **guage models**. *Preprint*, arXiv:2412.16926.

635 Janette B Benson. 2020. *Encyclopedia of infant and*
636 *early childhood development*. Elsevier.

637 Amanda Bertsch, Maor Ivgi, Emily Xiao, Uri Alon,
638 Jonathan Berant, Matthew R. Gormley, and Graham
639 Neubig. 2025. **In-context learning with long-context**
640 **models: An in-depth exploration**. In *Proceedings*
641 *of the 2025 Conference of the Nations of the Amer-*
642 *icas Chapter of the Association for Computational*
643 *Linguistics: Human Language Technologies (Volume*
644 *1: Long Papers)*, pages 12119–12149, Albuquerque,
645 New Mexico. Association for Computational Linguis-
646 tics.

647 Iñigo Casanueva, Tadas Temčinas, Daniela Gerz,
648 Matthew Henderson, and Ivan Vulić. 2020. **Efficient**
649 **intent detection with dual sentence encoders**. In *Pro-*
650 *ceedings of the 2nd Workshop on Natural Language*
651 *Processing for Conversational AI*, pages 38–45, On-
652 line. Association for Computational Linguistics.

653 Wenhui Chen, Xueguang Ma, Xinyi Wang, and
654 William W. Cohen. 2023. **Program of thoughts**
655 **prompting: Disentangling computation from reason-**
656 **ing for numerical reasoning tasks**. *Transactions on*
657 *Machine Learning Research*.

Karl Cobbe, Vineet Kosaraju, Mohammad Bavarian, Mark Chen, Heewoo Jun, Lukasz Kaiser, Matthias Plappert, Jerry Tworek, Jacob Hilton, Reichiro Nakano, Christopher Hesse, and John Schulman. 2021. Training verifiers to solve math word prob- lems. <i>arXiv preprint arXiv:2110.14168</i> .	658 659 660 661 662 663
Georges A Croes. 1958. A method for solving traveling- salesman problems. <i>Operations research</i> , 6(6):791– 812.	664 665 666
DeepSeek-AI, Daya Guo, Dejian Yang, Haowei Zhang, Junxiao Song, Ruoyu Zhang, Runxin Xu, Qihao Zhu, Shirong Ma, Peiyi Wang, Xiao Bi, Xiaokang Zhang, Xingkai Yu, Yu Wu, Z. F. Wu, Zhibin Gou, Zhi- hong Shao, Zhuoshu Li, Ziyi Gao, and 181 others. 2025. Deepseek-r1: Incentivizing reasoning capa- bility in llms via reinforcement learning . <i>Preprint</i> , arXiv:2501.12948.	667 668 669 670 671 672 673 674
Xinyu Guan, Li Lyra Zhang, Yifei Liu, Ning Shang, Youran Sun, Yi Zhu, Fan Yang, and Mao Yang. 2025. rstar-math: Small llms can master math rea- soning with self-evolved deep thinking . <i>Preprint</i> , arXiv:2501.04519.	675 676 677 678 679
Chi Han, Qifan Wang, Hao Peng, Wenhan Xiong, Yu Chen, Heng Ji, and Sinong Wang. 2024. LM- infinite: Zero-shot extreme length generalization for large language models . In <i>Proceedings of the 2024</i> <i>Conference of the North American Chapter of the</i> <i>Association for Computational Linguistics: Human</i> <i>Language Technologies (Volume 1: Long Papers)</i> , pages 3991–4008, Mexico City, Mexico. Association for Computational Linguistics.	680 681 682 683 684 685 686 687 688
Dan Hendrycks, Collin Burns, Saurav Kadavath, Akul Arora, Steven Basart, Eric Tang, Dawn Song, and Jacob Steinhardt. 2021. Measuring mathematical problem solving with the math dataset. <i>NeurIPS</i> .	689 690 691 692
Eduard Hovy, Laurie Gerber, Ulf Hermjakob, Chin- Yew Lin, and Deepak Ravichandran. 2001. Toward semantics-based answer pinpointing . In <i>Proceedings</i> <i>of the First International Conference on Human Lan-</i> <i>guage Technology Research</i> .	693 694 695 696 697
Janak Kapuriya, Manit Kaushik, Debasis Ganguly, and Sumit Bhatia. 2025. Exploring the role of diversity in example selection for in-context learning . <i>Preprint</i> , arXiv:2505.01842.	698 699 700 701
Takeshi Kojima, Shixiang Shane Gu, Machel Reid, Yu- taka Matsuo, and Yusuke Iwasawa. 2022. Large lan- guage models are zero-shot reasoners . In <i>Advances</i> <i>in Neural Information Processing Systems</i> .	702 703 704 705
Patrick Lewis, Ethan Perez, Aleksandra Piktus, Fabio Petroni, Vladimir Karpukhin, Naman Goyal, Heinrich Küttler, Mike Lewis, Wen-tau Yih, Tim Rock- täschel, and 1 others. 2020. Retrieval-augmented gen- eration for knowledge-intensive nlp tasks. <i>Advances</i> <i>in neural information processing systems</i> , 33:9459– 9474.	706 707 708 709 710 711 712

713	Tianle Li, Ge Zhang, Quy Duc Do, Xiang Yue, and Wenhua Chen. 2024. Long-context llms struggle with long in-context learning . <i>CoRR</i> , abs/2404.02060.	768
714		769
715		770
716	Yafu Li, Xuyang Hu, Xiaoye Qu, Linjie Li, and Yu Cheng. 2025. Test-time preference optimization: On-the-fly alignment via iterative textual feedback . <i>Preprint</i> , arXiv:2501.12895.	771
717		
718		
719		
720	Bill Yuchen Lin, Abhilasha Ravichander, Ximing Lu, Nouha Dziri, Melanie Sclar, Khyathi Chandu, Chandra Bhagavatula, and Yejin Choi. 2024. The unlocking spell on base LLMs: Rethinking alignment via in-context learning . In <i>The Twelfth International Conference on Learning Representations</i> .	772
721		773
722		774
723		775
724		776
725		
726	Jiachang Liu, Dinghan Shen, Yizhe Zhang, Bill Dolan, Lawrence Carin, and Weizhu Chen. 2022. What makes good in-context examples for GPT-3? In <i>Proceedings of Deep Learning Inside Out (DeeLIO 2022): The 3rd Workshop on Knowledge Extraction and Integration for Deep Learning Architectures</i> , pages 100–114, Dublin, Ireland and Online. Association for Computational Linguistics.	777
727		778
728		779
729		780
730		781
731		782
732		783
733		784
734	Man Luo, Xin Xu, Zhuyun Dai, Panupong Pasupat, Mehran Kazemi, Chitta Baral, Vaiva Imbrasaitė, and Vincent Y Zhao. 2023. Dr.icl: Demonstration-retrieved in-context learning . <i>Preprint</i> , arXiv:2305.14128.	785
735		
736		
737		
738		
739	Andrzej Maćkiewicz and Waldemar Ratajczak. 1993. Principal components analysis (pca). <i>Computers & Geosciences</i> , 19(3):303–342.	786
740		787
741		788
742	Leland McInnes, John Healy, and James Melville. 2018. Umap: Uniform manifold approximation and projection for dimension reduction. <i>arXiv preprint arXiv:1802.03426</i> .	789
743		790
744		
745		
746	MetaAI. 2024. Introducing meta llama 3: The most capable openly available llm to date .	791
747		792
748	Sewon Min, Xinxi Lyu, Ari Holtzman, Mikel Artetxe, Mike Lewis, Hannaneh Hajishirzi, and Luke Zettlemoyer. 2022. Rethinking the role of demonstrations: What makes in-context learning work? In <i>Proceedings of the 2022 Conference on Empirical Methods in Natural Language Processing</i> , pages 11048–11064, Abu Dhabi, United Arab Emirates. Association for Computational Linguistics.	793
749		794
750		795
751		796
752		797
753		798
754		799
755		
756	Bowen Peng, Jeffrey Quesnelle, Honglu Fan, and Enrico Shippole. 2024. YaRN: Efficient context window extension of large language models . In <i>The Twelfth International Conference on Learning Representations</i> .	800
757		801
758		802
759		803
760		804
761	Qwen, :, An Yang, Baosong Yang, Beichen Zhang, Binyuan Hui, Bo Zheng, Bowen Yu, Chengyuan Li, Dayiheng Liu, Fei Huang, Haoran Wei, Huan Lin, Jian Yang, Jianhong Tu, Jianwei Zhang, Jianxin Yang, Jiaxi Yang, Jingren Zhou, and 25 others. 2025. Qwen2.5 technical report . <i>Preprint</i> , arXiv:2412.15115.	805
762		806
763		807
764		808
765		809
766		810
767		811
768		812
769		
770		
771		
772		
773		
774		
775		
776		
777		
778		
779		
780		
781		
782		
783		
784		
785		
786		
787		
788		
789		
790		
791		
792		
793		
794		
795		
796		
797		
798		
799		
800		
801		
802		
803		
804		
805		
806		
807		
808		
809		
810		
811		
812		
813		
814		
815		
816		
817		
818		
819		
820		
821		
822		
823		
824		

825 Shunyu Yao, Dian Yu, Jeffrey Zhao, Izhak Shafran,
826 Thomas L. Griffiths, Yuan Cao, and Karthik R
827 Narasimhan. 2023. Tree of thoughts: Deliberate
828 problem solving with large language models. In
829 *Thirty-seventh Conference on Neural Information*
830 *Processing Systems*.

831 Yanzhao Zhang, Mingxin Li, Dingkun Long, Xin Zhang,
832 Huan Lin, Baosong Yang, Pengjun Xie, An Yang,
833 Dayiheng Liu, Junyang Lin, Fei Huang, and Jingren
834 Zhou. 2025. Qwen3 embedding: Advancing text
835 embedding and reranking through foundation models.
836 *Preprint*, arXiv:2506.05176.

A Algorithm for Curvature-Performance Correlation

To quantify the relationship between demonstration ordering smoothness and ICL performance, we develop Algorithm 1. The algorithm takes as input multiple orderings of demonstrations and their corresponding performance scores, and outputs a correlation coefficient between ordering smoothness and performance.

B Analysis of Similarity in Different LLM Types

Result in Figures 10 and 11 shows the performance comparison in different types of LLMs.

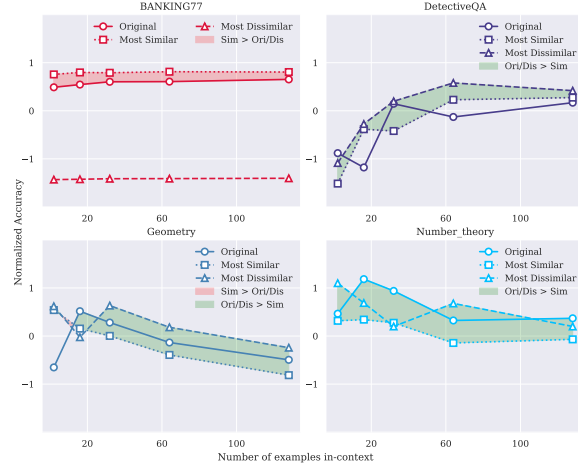


Figure 10: Performance with original (ori), similarity(sim) and dissimilar(dis) sets averaged across three non-reasoning LLMs. The area between the two sets is filled with colors, indicating the relative performance at each point.

C Prompt formatting and LLM performance for each task

C.1 SuperGlue

We evaluate the Winograd Schema Challenge (WSC) for coreference resolution, and the Choice of Plausible Alternatives (COPA) for open-domain commonsense causal reasoning. Both are formatted as a binary-label classification task. The prompt for inference is presented in Figure 12 and 13.

C.2 TREC

We evaluate the Text REtrieval Conference (TREC) Question Classification dataset with 50 fine class labels. The prompt for inference is presented in Figure 14.

Algorithm 1: Curvature-Performance Correlation Analysis

Input: For k different orderings:

- $E^{(1)}, E^{(2)}, \dots, E^{(k)}$: embedding matrices where $E^{(j)} = [e_1^{(j)}, e_2^{(j)}, \dots, e_N^{(j)}]^\top$ represents the j -th ordering of N demonstration embeddings

- $S = [S_1, S_2, \dots, S_k]$: performance scores for each ordering

Output: Correlation coefficient r between smoothness scores and performance scores

Initialize smoothness scores array

$$\mathbf{m} \leftarrow [0, 0, \dots, 0] \text{ of length } k$$

for each dimensionality reduction method

$$M \in \{PCA, UMAP\} \text{ do}$$

for $j = 1$ to k **do**

Step 1: Dimensionality reduction
 $\tilde{E}^{(j)} \leftarrow \text{ReduceDim}(E^{(j)}, M)$

Step 2: Compute curvature between consecutive demonstrations

$$\text{curvatures} \leftarrow []$$

for $i = 2$ to $N - 1$ **do**

$$\mathbf{v}_1 \leftarrow \tilde{\mathbf{e}}_i^{(j)} - \tilde{\mathbf{e}}_{i-1}^{(j)}$$

$$\mathbf{v}_2 \leftarrow \tilde{\mathbf{e}}_{i+1}^{(j)} - \tilde{\mathbf{e}}_i^{(j)}$$

if $\|\mathbf{v}_1\| > 0$ and $\|\mathbf{v}_2\| > 0$ **then**

$$\cos \theta_i \leftarrow \frac{\mathbf{v}_1 \cdot \mathbf{v}_2}{\|\mathbf{v}_1\| \|\mathbf{v}_2\|}$$

$$\theta_i \leftarrow \arccos(\cos \theta_i)$$

Append θ_i to curvatures

Step 3: Compute smoothness score

$$\bar{\theta}^{(j)} \leftarrow \text{mean}(\text{curvatures})$$

$$\text{score}_M^{(j)} \leftarrow \frac{1}{1 + \bar{\theta}^{(j)}}$$

Step 4: Weighted combination (equal weighting for PCA and UMAP)

$$\mathbf{m}[j] \leftarrow \mathbf{m}[j] + 0.5 \times \text{score}_M^{(j)}$$

Step 5: Compute correlation

$$r \leftarrow \text{PearsonCorrelation}(\mathbf{m}, S)$$

return r

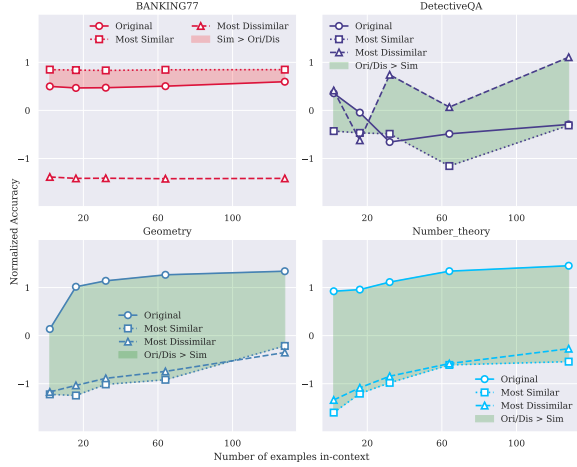


Figure 11: Performance with original (ori), similarity(sim) and dissimilar(dis) sets averaged across two reasoning LLMs. The area between the two sets is filled with colors, indicating the relative performance at each point.

C.3 BANKING77

We evaluate the BANKING77 dataset with 77 fine-grained intents in the banking domain. The prompt for inference is presented in Figure 15.

C.4 NLU

We evaluate the NLU dataset with 68 fine-grained intents in the conversational domain. The prompt for inference is presented in Figure 16.

C.5 GSM8K

We evaluate the GSM8K dataset for grade school math word problems. The prompt for inference is presented in Figure 17.

C.6 MATH

We evaluate the Mathematics Aptitude Test of Heuristics (MATH) dataset for mathematics competition problems, including the question types of counting_and_probability, prealgebra, geometry, precalculus, number_theory and algebra. The prompt for inference is presented in Figure 18.

Given a query, answer yes or no to the query.

The predicted answer must come from the demonstration examples with the exact format. The examples are as follows:

Question: In the sentence “{text₁ }”, does the pronoun ‘{span2_text₁}’ refer to {span1_text₁}?
Answer: {answer₁}

...

Question: In the sentence “{text_n }”, does the pronoun ‘{span2_text_n}’ refer to {span1_text_n}?
Answer: {answer_n}

Now predict the answer for the following query:

Question: In the sentence “{text_i }”, does the pronoun ‘{span2_text_i}’ refer to {span1_text_i}?

reply in the following format:
‘Answer: [yes | no]’

Figure 12: Prompt for WSC task

Answer in A or B.

The predicted answer must come from the demonstration examples with the exact format. The examples are as follows:

Premise: {premise₁}
Question: What is the {question₁} for this?
Options:
A. {choice1₁}
B. {choice2₁}
Answer: {answer₁}

...

Premise: {premise_n}
Question: What is the {question_n} for this?
Options:
A. {choice1_n}
B. {choice2_n}
Answer: {answer_n}

Now predict the answer for the following query:

Premise: {premise_i}
Question: What is the {question_i} for this?
Options:
A. {choice1_i}
B. {choice2_i}

reply in the following format:
‘Answer: [A | B]’

Figure 13: Prompt for COPA task

Given a question, predict the label of the question. You can only make predictions from the following categories:
{LIST_OF_CATEGORIES}
Please predict the label of the FINAL question with the provided demonstration example queries as follows:

question: {question₁}
label: {label₁}
...
question: {question_n}
label: {label_n}

Now predict the answer for the following query:

question: {question_i}

reply in the following format:
'label: [category_name]'

Figure 14: Prompt for TREC task

Given a question, predict the label of the question. You can only make predictions from the following categories:
{LIST_OF_CATEGORIES}
Please predict the intent category of the FINAL query with the provided demonstration example queries as follows:

service query: {question₁}
intent category: {label₁}
...
service query: {question_n}
intent category: {label_n}

Now predict the intent category for the following query:

service query: {question_i}

reply in the following format:
'intent category: [category_name]'

Figure 15: Prompt for BANKING77 task

Given a question, predict the label of the question. You can only make predictions from the following categories:
{LIST_OF_CATEGORIES}
Please predict the intent category of the FINAL utterance with the provided demonstration example queries as follows:

utterance: {question₁}
intent category: {label₁}
...
utterance: {question_n}
intent category: {label_n}

Now predict the intent category for the following utterance:

utterance: {question_i}

reply in the following format:
'intent category: [category_name]'

Figure 16: Prompt for NLU task

In the end of the response, add a summary ‘The answer is [answer].’

Q: {question₁}
A: {CoT₁} {answer₁}

...

Q: {question_n}
A: {CoT_n} {answer_n}

Q: {question_t}
A: Let’s think step by step.

Figure 17: Prompt for GSM8K task

Write a response that appropriately completes the request and wrap the final answer inside \boxed{ }.

Problem: {question₁}
Solution: {CoT_with_answer₁}

...

Problem: {question_n}
Solution: {CoT_with_answer_n}

Problem: {question_t}
Solution: Let’s think step by step.

Figure 18: Unified prompt for MATH task